Erschienen in: Nineteenth European Photovoltaic Solar Energy Conference : proceedings of the international conference held in Paris, France, 7 - 11 June 2004 ; Vol. 1 / Hoffmann, Winfried et al. (Hrsg.). - München [u.a.] : WIP, 2004. - S. 709-712. - ISBN 3-936338-14-0

DETERMINATION OF THE OXYGEN, CARBON AND VACANCY CONCENTRATION IN SOLAR-GRADE SILICON AND CORRELATION WITH THE HYDROGEN DIFFUSIVITY

D. Karg[1], H. Charifi[1], G. Pensl[1], M. Schulz[1] and G. Hahn[2]
[1] University of Erlangen, Institute of Applied Physics, Staudtstraße 7, 91058 Erlangen, Germany
[2] University of Konstanz, Department of Physics, P.O.Box X916, 78457 Konstanz, Germany
Tel: +49-9131 85-28429, Fax: +49-9131 85-28423, Email: dieter.karg@physik.uni-erlangen.de

ABSTRACT: Platinum (Pt)-diffusion is a convenient method to monitor vacancy profiles in silicon (Si). We have applied this method for the determination of vacancy profiles of Ribbon Growth on Substrate (RGS) silicon prior to and subsequent to phosphorus (P)-diffusion and for the determination of the vacancy concentration [Vac] in other as-grown solar-grade Si materials. [Vac] prior to and subsequent to P-diffusion of RGS was compared to the concentration of oxygen (O), carbon (C), density of precipitates (O, C) and to the diffusivity of hydrogen (H). Based on our results, it turns out that [Vac] is not directly correlated with the interstitial oxygen concentration [O_i] in as-grown Si. However, the decrease of [Vac] subsequent to a P-diffusion at 850°C is caused by generation of precipitates containing C and O. It is assumed that precipitates are also responsible for the reduced H diffusivity by trapping H atoms. In addition, in vacancy-rich, precipitation-lean Si, the H diffusivity can be enhanced by vacancies, dissociating immobile H_2 molecules.
Keywords: Multi-Crystalline, Passivation, Defects

1 INTRODUCTION

Fabrication of efficient solar cells on commercial Si substrates involves gettering and passivation to slow down deleterious effects of impurities and defects. Gettering is extensively used for optimization of P-diffusion and aluminum (Al)-alloying needed for the formation of p-n junction and ohmic contacts. Even after gettering, significant concentrations of impurities and defects remain electrically active in the solar cell. Therefore, most of the Si solar cell manufacturers apply hydrogenation to passivate remaining impurities and defects.

One promising hydrogenation method is the deposition of a H-rich PECVD SiN layer followed by a firing step in the range of 800°C to release the H-atoms into the Si bulk. This method is commonly used in industrial production of mc-Si solar cells. It is an experimental fact that the effective H diffusivity depends on the silicon material (see e.g. [1, 2, 7, 8]). For example, as compared to EFG Si [3] the H diffusivity is significantly slower in RGS Si [4]. In a previous publication [5], we suppose that a high [Vac] is responsible for fast H-diffusion in EFG Si. As predicted by [6], it is assumed that vacancies enhance the H diffusivity by dissociating immobile H_2 molecules. Further on, a H diffusions mechanism via Vac-H pairs has been proposed by [22] which can also explain a high H diffusivity. On the other hand, the authors of [7, 8] assume that interstitial oxygen (O_i) decreases the effective H diffusivity and the reason for the higher passivation rate in EFG Si is the relatively low [O_i] < 10^{17}cm^{-3}. In this study, we will combine these two assumptions, demonstrating the simultaneous effect of oxygen and vacancies on the hydrogen diffusivity in solar-grade silicon.

We investigate three differently processed RGS wafers and compare [Vac] prior to and subsequent to P-diffusion to the concentration of interstitial oxygen (O_i), substitutional carbon (C_s), O and C precipitates and to the diffusivity of H. In addition, other Si materials (e.g. block-cast mc-Si [9], String Ribbon Si [10], FZ-Si and Cz-Si) were investigated. To obtain [Vac] in solar-grade Si, vacancy profiles were determined by the platinum (Pt)-diffusion method. The Pt-diffusion method was developed at the Fraunhofer Institute of Integrated Circuits in Germany [11]. [O_i] and [C_s] are determined by IR spectroscopy. SIMS profiles of the H diffusivity and the total oxygen concentration [O] of the three RGS wafers were obtained from R. Ginige and K. Cherkaoui (see also [2]).

2 PLATINUM DIFFUSION

Pt can dissolve interstitially and substitutionally in Si. The solubility of substitutional Pt (Pt_s) is much larger than the solubility of interstitial Pt (Pt_i), whereas the interstitial Pt diffuses fast in comparison to substitutional Pt. For that reason, there is a continuous exchange of Pt atoms between interstitial (Pt_i) and substitutional (Pt_s) lattice sites during the diffusion of Pt. This exchange can take place via the Frank-Turnbull mechanism [20], involving vacancies (Vac), or via the kick-out mechanism [21] involving Si interstitials (Si_i). The reaction of the Frank-Turnbull mechanism is

$$Pt_i + Vac \underset{k_2}{\overset{k_1}{\Leftrightarrow}} Pt_s \qquad (1)$$

and the reaction of the kick-out mechanism leads to

$$Pt_i \underset{k_4}{\overset{k_3}{\Leftrightarrow}} Pt_s + Si_i \ . \qquad (2)$$

k_1, k_2, k_3 and k_4, are the reaction rates of the corresponding forward and reverse direction, respectively. It was shown that Pt in Si mainly diffuses via the Frank-Turnbull mechanism at temperatures up to 750°C and for diffusion times less or equal to 1h and initial vacancy concentrations [Vac(t=0)] higher than 10^{11}cm^{-3} [18].

When local equilibrium is established for the Frank-Turnbull mechanism, [Vac(t=0)] and [Pt_s] are related by

$$[Vac(t=0)] = [Pt_s] \times \left(1 + [Vac^{eq}] / [Pt_s^{eq}]\right). \qquad (3)$$

[Vac^{eq}] and [Pt_s^{eq}] are the equilibrium concentrations of vacancies and Pt_s, respectively.

3 EXPERIMENTAL

The main goal of the Pt-diffusion is to determine the vacancy profile in Si materials. According to [18], [Vac^{eq}] and [Pt$_s^{eq}$] are given by

$$[Vac^{eq}] = 1.7 \times 10^{21} \cdot (-2.00eV/kT) \text{ cm}^{-3} \quad (4)$$

and

$$[Pt_s^{eq}] = 6.4 \times 10^{29} \cdot (-3.45eV/kT) \text{ cm}^{-3}. \quad (5)$$

According to equations (3), (4) and (5), [Vac(t=0)] and [Pt$_s$] are given by [Vac(t=0)] = [Pt$_s$] × 1.05 at 730°C, respectively.

In this work, [Pt$_s$] is determined by deep level transient spectroscopy (DLTS). DLTS is a very sensitive method, which allows the accurate measurement of [Pt$_s$]; the detectable [Pt$_s$] is limited by the ratio [Pt$_s$]/[B]=10^{-1} to 10^{-5} related to the boron (B)-concentration. Pt$_s$ has three defect levels in the Si band gap, an acceptor-like, a donor-like and a double donor-like [19]. In p-type Si, the Pt$_s$ donor level at E_V+0.33eV and the double donor level at E_V+0.067eV, in n-type Si, the acceptor level E_C-0.23eV can be detected by DLTS. In this work, the peak heights of the donor level (p-type) and of the acceptor level (n-type) are used for the determination of [Pt$_s$], respectively.

The experiments were performed on RGS Si prior to and subsequent to P-diffusion at 850°C for 20min and on as-grown HEM, Baysix® Si, String Ribbon Si, FZ-Si and Cz-Si. The wafers were cut into samples with a size of 2 × 1cm^2, each. The samples were exposed to a standard cleaning procedure. Pt was deposited on the surface by dipping the samples for 2 min in an aqueous Pt standard solution. The diffusions were performed in a conventional diffusion furnace under nitrogen ambient at T = 730°C for t = 30min, followed by a fast ramp down of the temperature. Subsequent to the diffusion, the surface of the samples was cleaned by aqua regia and etched by a modified CP4-etch. The next step is a 150µm deep angle polishing (approx 1°) of one surface (front or back) of the samples (see Fig.1). The initial thickness of the samples is approximately 300µm. After angle polishing, Ti Schottky contacts (area = 0.4mm^2) and a large ohmic Al contact were evaporated on the angle polished surface and on the backside, respectively (see Fig. 1).

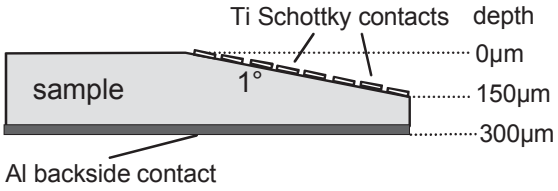

Fig. 1 Cross section of angle polished samples with Ti Schottky contacts and a large ohmic aluminum backside contact.

Finally, [Pt$_s$] is determined by the height of the DLTS signal of the Pt$_s$ donor level. ´

[O$_i$] and [C$_s$] of the as-grown and P-diffused RGS wafers, shown in Table 1, are determined by IR absorption measurements.

Table 1: [O$_i$] and [C$_s$] of as-grown and P-diffused RGS Si samples: RGS #1, RGS #2 and RGS #3.

	as-grown		subsequent to P-diffusion	
	[O$_i$] [10^{18}cm^{-3}]	[C$_s$] [10^{18}cm^{-3}]	[O$_i$] [10^{18}cm^{-3}]	[C$_s$] [10^{18} cm^{-3}]
RGS #1	0.75	3.1	0.3	2.7
RGS #2	0.3	2.7	0.3	2.8
RGS #3	2.9	2.6	0.4	0.9

4 RESULTS

4.1 Vacancy profiles of RGS Si

The effect of P-diffusion (heat treatment at 850°C for 20min) on the vacancy profile in three RGS samples (RGS #1, RGS #2 and RGS #3) with different [O$_i$] was investigated (see also Table 1). Figure 2 shows the vacancy profile of RGS #1 prior to and subsequent to P-diffusion. A homogeneous vacancy profile of (1-3) × 10^{13} cm^{-3} was measured in the sample prior to P-diffusion. Meanwhile, no Pt-related DLTS peak was observed in the P-diffused sample, which indicates that [Vac] is below the detection limit of 5 × 10^{11} cm^{-3}.

Figure 3 shows the vacancy profile of RGS #2 prior to subsequent to P-diffusion. The vacancy profiles indicate that the vacancies are roughly homogeneously distributed in sample RGS #2 prior to subsequent to P-diffusion. In addition, [Vac] does not significantly change during P-diffusion .

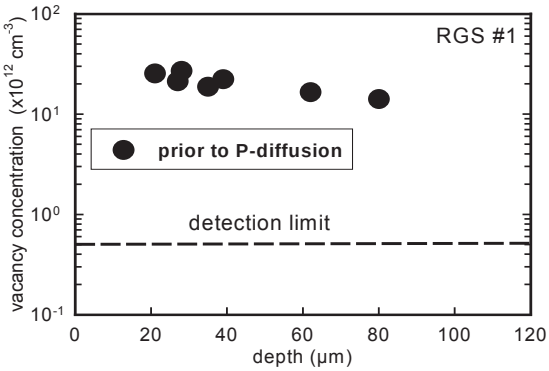

Fig. 2 Vacancy profile of RGS #1 prior to P-diffusion. Subsequent to P-diffusion, [Vac] is below the detection limit of 5 × 10^{11} cm^{-3} (see dashed line).

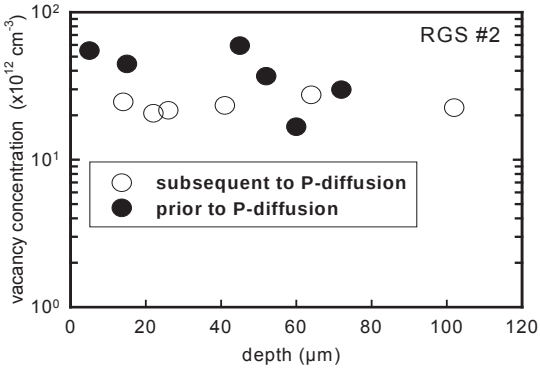

Fig. 3 Vacancy profile of RGS #2 prior to and subsequent to P-diffusion.

In RGS #3, [Vac] is below the detection limit of approximately 10^{12} cm^{-3} at all contacts investigated prior to and subsequent to P-diffusion.

4.2 Vacancy concentration in HEM, String Ribbon, FZ-Si and Cz-Si

A comparison of [Vac] in actual HEM and in older Baysix® wafers (1999) in the as-grown state was conducted. The block diagram (Fig. 4) shows the [Vac] distribution in n- and p-type HEM wafers. [Vac] is inhomogeneously distributed in the p- and n-type HEM ingots with a, compared to Baysix wafers ([Vac] < $5 \times 10^{11}cm^{-3}$ [5]) significantly higher concentration of (3-10) $\times 10^{12}cm^{-3}$.

For a comparison, [Vac] of as-grown SR-Si, FZ-Si and Cz-Si was determined, too. The obtained values are shown in Table 2. In contrast to EFG-Si ([Vac]=(1-2) $\times 10^{13}$ cm^{-3} [5]), the fluctuations of [Vac] in SR-Si are larger ([Vac] = (4-30) $\times 10^{12}$ cm^{-3}).

Table 2 [Vac] of different solar-grade Si materials in the as-grown state.

silicon	HEM	Baysix [5]	EFG [5]	SR	FZ (N-doped)	Cz
[Vac] × $10^{12}cm^{-3}$	3-10	< 0.5	10-20	4-30	30-50	0.5-1

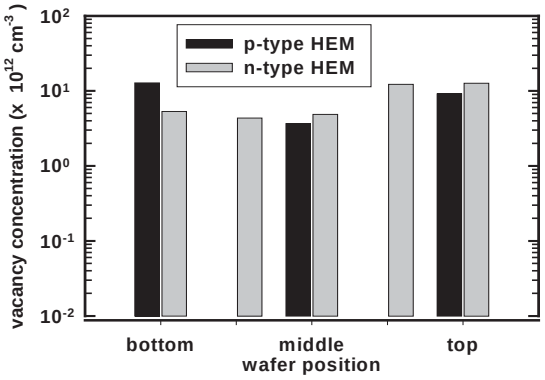

Fig. 4 [Vac] in n- and p-type HEM wafers at different positions of the ingot.

5 DISCUSSION

5.1 Oxygen, carbon and intrinsic point defects

The [Vac] and [Si_i] in Si materials strongly depend on the crystal growth conditions (e.g. growth rate, axial temperature gradient), on [O_i] and [C_s], on the nucleation and growth of O and C precipitates and also on the amount of extended defects (e.g. dislocations and microdefects) (see e.g. [12-16]). O_i expands the lattice and generates vacancies, C_s contracts the lattice and generates Si_i. Oxygen precipitation occurs readily in the Si crystal. During oxygen precipitate nucleation and growth vacancies are consumed and/or Si_i are emitted, both leading to a vacancy depletion in the Si crystal. C precipitation in Si is a difficult process, which takes place only in the presence of a sufficiently high supersaturation of O or Si_i. During the C precipitation Si_i are trapped. If both, C_s and O_i, are present in large supersaturation, a fast co-precipitation of C and O occurs (ratio approx. 1:2) (see [17]). Up to now, it is not exactly known, whether C is directly involved in precipitates, is located in the strain field of the precipitates or simply traps Si_i. For example, in RGS #1 and #3 precipitation of O and C occurs. Subsequent to phosphorus diffusion at 850°C for 20min, the loss ratios of C_s and O_i are 1:1.1 and 1:1.5, respectively (see table 1). In both cases more C_s is precipitated than expected for the predicted ratio of 1:2. It is assumed that C also forms clusters with Si_i (see e.g. [14]). On the other hand, [O_i] and [C_s] of RGS #2 do not significantly change during P-diffusion, assuming that no appreciable additional precipitation occurs.

5.2 Correlation of the vacancy, oxygen and carbon concentration with the H diffusivity

In a previous publication [5], compared to other solar-grade Si, we suppose that the high [Vac] is responsible for the fast H-diffusion in EFG Si. As predicted by Estreicher et al. [6], it was assumed that vacancies can enhance the H diffusivity by dissociating immobile H_2 molecules. On the other hand, the authors of [7, 8] suggest that O_i decreases the effective H diffusivity and the reason for the higher passivation rate in EFG Si is the relatively low [O_i] < $10^{17}cm^{-3}$. Sopori et al. [1] suppose that the H diffusivity depends on the concentration of impurities like O and C.

In another paper on this conference, H-diffusion experiments of the RGS wafers RGS #1, #2 and #3 are displayed [2]. In wafer RGS #2, the effective H diffusivity is higher and the trapped [H] is lower in comparison to the other RGS wafers. Our experimental results have demonstrated that RGS #2 is the only investigated wafer without a significant decrease in [C_s] and [O_i] subsequent to phosphorus diffusion, resulting in a low density of generated precipitates (see Table 1). Additionally, compared to RGS #1, [Vac] in RGS #2 only moderately decreases during phosphorus diffusion (see Fig. 3). On the other hand, [Vac] in RGS #1, a wafer with higher oxygen concentration than RGS #2, can not be detected subsequent to phosphorus diffusion (see Fig. 2). It is assumed that the strong decrease of vacancies subsequent to P-diffusion is caused by oxygen precipitation in RGS #1 or, in other words, the vacancies are absorbed by the precipitates. In RGS #3, a wafer with a still higher interstitial oxygen concentration, [Vac] is below the detection limit (approx. $10^{12}cm^{-3}$) prior to and subsequent to phosphorus diffusion. This can be explained by a sufficient high precipitate density, which was already present prior to the P-diffusion and which absorbed most of the vacancies, generated during crystal growth.

By considering all details, we suggest that the correlation between O, C, vacancies and H diffusivity is the following:

- [Vac] is not directly correlated with [O_i] in Si
- The decrease of [Vac] subsequent to heat treatments at 850°C is related to the generation of precipitates (C, O).
- Precipitates reduce the H diffusivity by trapping H.
- In general, the relatively slow H diffusion in RGS is caused by the high density of precipitates.
- The comparatively faster H diffusivity in RGS #2, as compared to RGS #1 and #3, is caused by the lower density of precipitates.

- In vacancy-rich, precipitation-lean Si, the H diffusivity can be enhanced by vacancies, dissociating immobile H_2 molecules.
- The fast H diffusivity of EFG is caused by the, compared to RGS Si, low density of oxygen-containing precipitates and by the high [Vac].

6 CONCLUSION

[Vac] is not directly correlated with [O_i] in Si, however, decreases with increasing density of precipitates (O, C). The varying H diffusivity in solar-grade materials is explained by a different density of precipitates. In vacancy-rich, precipitation-lean Si, the H diffusivity can, in addition, be enhanced by vacancies, dissociating immobile H_2 molecules.

7 ACKNOWLEDGEMENTS

The authors would like to thank R. Ginige and K. Cherkaoui for SIMS measurements and A. Schönecker, M. Ghosh and A. Gabor for the supply of solar-grade Si. This work is partly supported by the German Bundesministerium für Umwelt, Naturschutz und Reaktorsicherheit (BMU) under contract number 0329846 (project ASiS).

8 REFERENCES

[1] B. Sopori, Y. Zhang and R. Reedy, *29th PVSC*, (IEEE, New Orleans, 2002), p. 222
[2] G. Hahn, D. Sontag, S. Seren, A. Schönecker, A.R. Burgers, R. Ginige, K. Cherkaoui, D. Karg, H. Charifi, *19th EC PVSEC*, (Paris 2004), to be published
[3] J. P. Kalejs in: Silicon Processing for Photovoltaics, Vol. II. Eds. C. P. Khattak and K. V. Ravi (Elsevier Amsterdam 1987) ch. 4
[4] H. Lange, I.A. Schwirtlich, J. Crystal Growth, **104**, 108 (1990)
[5] D. Karg, G. Pensl, M. Schulz, *3rd WCPEC*, (Osaka 2003), p. 1112
[6] S.K. Estreicher, J.L. Hastings, P.A. Fedders, *Physical Review B*, **57**, R12663 (1998)
[7] G. Hahn, C. Haessler, M. Langenkamp, *17th EC PVSEC*, (Munich 2001), p. 1371
[8] T. Pernau, G. Hahn, M. Spiegel, G. Dietsche, *17th EC PVSEC*, (Munich 2001), p. 1764
[9] W. Koch, W. Krumbe, I. A. Schwirtlich, Proc. 11th EC PVSEC, Montreux, 518 (1992)
[10] R.L. Wallace, J.I. Hanoka, A. Rohatgi, G. Crotty, Sol. Energy Mater. Sol. Cells, **48**, 179 (1997)
[11] H. Zimmermann and H. Ryssel, *Appl. Phys. A*, **55**, 121 (1992)
[12] J.P. Kalejs, J. Crystal Growth, **128**, 298 (1993)
[13] B. Pivac, M. Amiotti, A. Borghesi, A. Sassella, J. Kalejs, J. Appl. Phys. **71**, 3785 (1992)
[14] W.J. Taylor, T.Y. Tan, U. Gösele, Appl. Phys. Lett., **62**, 3336 (1993)
[15] V.V. Voronkov, R. Falster, J. Electrochem. Soc., **149**, G167 (2002)
[16] V.V. Voronkov, R. Falster, J. Appl. Phys. **91**, 5802 (2002)
[17] Q. Sun, K.H. Yao, J. Lagowski, H.C. Gatos, J. Appl. Phys. **67**, 4313 (1990)
[18] M. Jakob, P. Pichler, H. Ryssel, R. Falster, J. Appl. Phys., **82**, 182 (1997)
[19] H. Zimmermann, H. Ryssel, Appl. Phys. Lett., **58**, 499 (1991)
[20] F.C. Frank, D. Turnbull, Phys. Rev., 104, 617 (1956)
[21] U. Gösele, W. Frank, A. Seeger, Appl. Phys. 23, 361 (1980)
[22] M.A. Roberson, S.K. Estreicher, Phys. Rev. B, **49**, 17040 (1994)